A Wavelet Network Control Method for Disk Drives

C. M. Chang and T. S. Liu

***Abstract*—This paper proposes a wavelet network control method to online learn and cancel repetitive errors in disk drives. In contrast to Fourier transforms, wavelet transforms can provide detailed local information of signals. Based on the wavelet transform, wavelets can approximate any finite energy function. This paper proposes wavelet networks to approximate periodic functions. Accordingly, a wavelet network controller is developed to eliminate repetitive error caused by repetitive disturbance. Experiments for flying height control of a disk drive system are implemented to demonstrate the present method in comparison with another method using Fourier series based network control.**

***Index Terms*—Bender, disk drive, flying height control, PZT, repetitive error, wavelet network (WN), wavelet theory.**

I. Introduction

TRACKING control commonly appears in servomechanisms where high accuracy is demanded. Tracking errors can be classified into two types: repetitive and nonrepetitive errors. In general, repetitive tracking errors appear due to tracking periodic inputs or disturbances. Many methods have been proposed to deal with repetitive errors, such as internal-model-based repetitive control, observer-based learning control [1], and neural-network-based control techniques [2]. On the other hand, the wavelet transform emerges as a new powerful tool for signal processing and function approximation. Comparing with the short-time Fourier transform that gives signal information with a fixed time window, the wavelet transform gives detailed local information of a signal by translating and narrowing a time window for detecting high-frequency behavior while widening one for investigating low-frequency behavior. Hence, on a time-frequency plane, wavelet transforms achieve a better compromise between time and frequency domains [3]. The repetitive error due to spindle motor rotation of disk drives lies in the low-frequency region. Wavelets with a large time window can detect low-frequency information of the repetitive error, while maintaining good time localization property. Inspired by the wavelet transform theory and neural networks, to deal with disk drives, this paper develops a wavelet network controller using wavelets to generate periodic control signals that can cancel repetitive errors. Experimental results and simulation results are presented to demonstrate the effectiveness of the proposed method.

Manuscript received February 11, 2004. Manuscript received in final form September 7, 2005. Recommended by Associate Editor D. W. Repperger. This work was supported by the National Science Council in Taiwan, R.O.C., by Grant NSC94-2752-E009-009-PAE.

The authors are with the Department of Mechanical Engineering, National Chiao Tung University, Hsinchu 30010, Taiwan, R.O.C. (e-mail: tsliu@mail.nctu.edu.tw).

Digital Object Identifier 10.1109/TCST.2005.860523

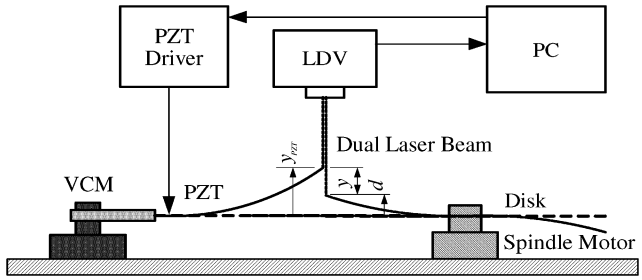

Fig. 1. Experimental setup for PZT-disk system.

II. PZT-Disk System

In order to control the flying height of a pickup head to follow disk deformation of a disk drive in this paper, an apparatus including a PZT bender and a disk drive is shown in Fig. 1. The control algorithm is executed on a PC and its output via a PZT driver controls the bending displacement $y_{\rm PZT}$ at the tip of the PZT bender. When the spindle motor rotates at a constant speed, the disk surface deformation d is composed of a repetitive component d_r and a nonrepetitive component $d_{\rm nr}$. The flying height $y = y_{\rm PZT} - d$ is measured by using a laser Doppler vibrometer as the feedback signal.

The block diagram of the present control system is depicted in Fig. 2 where r denotes the desired flying height. The wavelet network (WN) control signal r_c is used to cancel repetitive disk surface deformation d_r that causes repetitive errors. During disk rotation, the disk surface deformation d is treated as an output disturbance in controlling bending displacement of the PZT bender tip to follow the disk surface. The PZT driver that amplifies the control voltage u_c can be treated as a constant gain K. A linear model $P(s)$ of the plant, i.e., the PZT bender, is identified and Bode plots of open-loop gain $KP(s)$ are depicted in Fig. 3. To stabilize the closed-loop system, a compensator $C(s)$ is designed so that $KC(s)P(s)$ becomes a type 1 system with the gain margin and phase margin of 20.5 dB and 67.7 deg, respectively. According to Fig. 2, the flying height of the PZT bender tip is expressed by

$$Y(s) = \frac{KC(s)P(s)R(s)}{1+KC(s)P(s)} - \frac{D_{\rm nr}(s)}{1+KC(s)P(s)} + \frac{KC(s)P(s)R_c(s) - D_r(s)}{1+KC(s)P(s)}. \quad (1)$$

Dealing with the third term on the right-hand side (RHS), in order to cancel the repetitive disturbance $d_r(t)$, the WN controller proposed in the next section is trained until its control signal $r_c(t)$ achieves $R_c(s) = D_r(s)/KC(s)P(s)$. Accordingly, the repetitive error caused by the repetitive disturbance

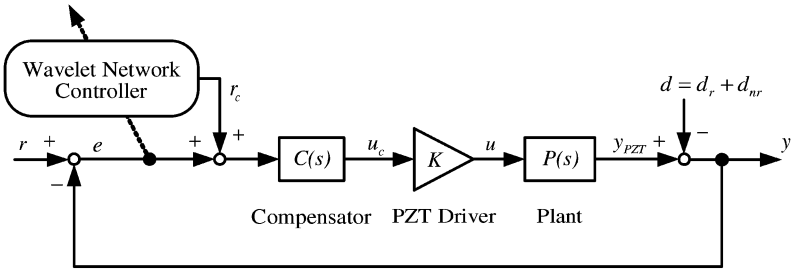

Fig. 2. Block diagram of PZT-disk system.

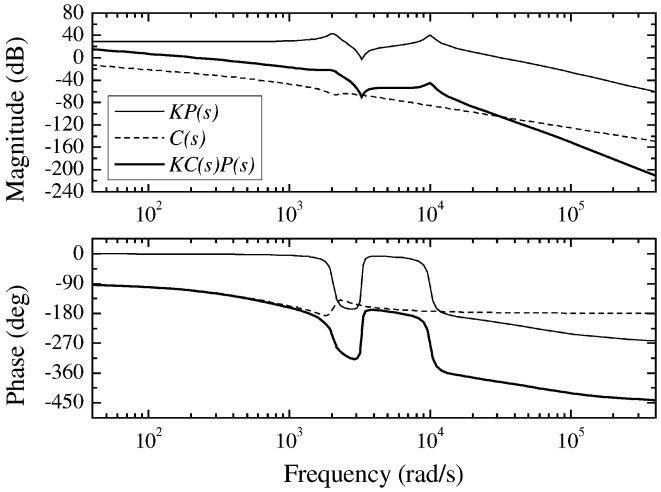

Fig. 3. Compensator design in frequency domain.

can be eliminated and the flying height y depends on the desired flying height r subject to remaining nonrepetitive disturbance $d_{\rm nr}$.

III. Wavelet Network Control

In contrast to Fourier series expansions that express a periodic function in terms of trigonometric series, a wavelet series expansion expresses a finite energy function with a series set obtained by dilating and translating a zero-mean mother wavelet. Concerning the wavelet theory, mathematical foundations of wavelets were developed by Grossmann and Morlet [4]. Mallat [5] presented wavelet representations to approximate signals at a given resolution. The wavelet transform and the short-time Fourier transform (STFT) were compared by Daubechies [3]. The wavelet transforms better compromise in localization between time and frequency domains than the STFT. The wavelet network was proposed by Zhang and Benveniste [6] to approximate nonlinear functions. Delyon *et al.* [7] carried out accuracy analysis to approximate a continuous function using a wavelet network. In contrast to wavelets, a biased wavelet has a nonzero mean and can better reproduce signal components that are in the low-frequency region on the time-frequency plane since the nonzero mean enlarges low-frequency gain [8]. In this paper for disk drives, the spindle motor speed is 90 Hz which lies in the low-frequency region among 5-kHz measurement bandwidth in experiments. Hence, this paper employs biased rather than unbiased wavelets and a wavelet network controller is developed.

A. Biased Wavelet

A set $\boldsymbol{H}$ of biased wavelets $h_{a,b,c}(t)$ is defined by [8]

$$\boldsymbol{H} = \left\{ h_{a,b,c}(t) = |a|^{-1/2} \left[\psi\left(\frac{t-b}{a}\right) + c\sigma\left(\frac{t-b}{a}\right) \right], a \in R - \{0\}, b, c \in R \right\} \quad (2)$$

where $\psi \in L^2(R)$, i.e., $\int_{-\infty}^{\infty} |\psi(t)|^2\, dt < \infty$, denotes a mother wavelet and a and b are dilation and translation parameters of the biased wavelet, respectively. In contrast to wavelets, biased wavelets have an adjustable nonzero mean bias function $\sigma \in L^2(R)$ that improves representation capability of biased wavelet expansions, which better reproduce signal components in the low-frequency region on the time-frequency plane than wavelet expansions. The set $\boldsymbol{H}$ reduces to a wavelet set $\boldsymbol{\Psi}$ when the bias parameter c is set to zero, since $h_{a,b,0} = \psi_{a,b}$. Any finite energy function $f(t) \in L^2(R)$ can be expanded using the biased wavelet set $\boldsymbol{H}$ or the wavelet set $\boldsymbol{\Psi}$. In general, $\psi_{a,b}$ are not linearly independent, which means that both $\boldsymbol{H}$ and $\boldsymbol{\Psi}$ are frames for $L^2(R)$ rather than bases.

B. Wavelet Network Approximation

Based on the wavelet transform, the wavelet network proposed in [6] is of the form

$$f_N(t) = \sum_{i=1}^{N} q_i \psi\left(\frac{t-b_i}{a_i}\right) + \theta \quad (3)$$

where $\psi(t)$ is a wavelet, a_i and b_i denote dilation and translation parameters, respectively, q_i are weightings, and θ is an offset to help deal with nonzero mean functions. In order to achieve better approximation, particularly for signals that lie in the low frequency region on the time-frequency plane, this paper proposes a biased wavelet network on the basis of biased wavelet sets $h_i(t) = \psi(t) + c_i\sigma(t)$, defined as

$$\begin{aligned} f_N(t) &= \sum_{i=1}^{N} q_i h_i\left(\frac{t-b_i}{a_i}\right) + \theta \\ &= \sum_{i=1}^{N} q_i \left(\left(\frac{t-b_i}{a_i}\right) + c_i \left(\frac{t-b_i}{a_i}\right) \right) + \theta. \end{aligned} \quad (4)$$

This paper will use (4) in constructing biased wavelet networks.

A Mexican hat wavelet $\psi(t) = (1 - t^2)\exp(-t^2/2)$ is chosen as the mother wavelet and the bias function is defined

as a Gaussian function [8] $\sigma(t) = \exp(-t^2/2)$. Substituting into (2) yields a biased wavelet

$$h(\tau) = \psi(\tau) + c\sigma(\tau) = (1 + c - \tau^2)\exp(-\tau^2/2) \quad (5)$$

where $\tau = (t - b)/a$.

C. Periodic Function Approximation

The wavelet networks cannot be directly applied to approximate a periodic function $g(t)$, since $g(t)$ is not a finite energy function, i.e., $g(t) \notin L^2(R)$. However, if the periodic function $g(t)$ with a period $2l$ satisfies an integration condition

$$\int_{-l}^{l} |g(t)|^2 < \infty \quad (6)$$

one can find a finite energy function $f(t)$ that satisfies $f(t) = g(t)$ when $-l \le t < l$ and has a wavelet network approximation $f_N(t)$. Hence, the periodic function $g(t)$ can be rewritten as

$$\begin{cases} g(t) = f(t), & -l \le t < l \\ g(t + 2l) = g(t), & \text{otherwise} \end{cases} \quad (7)$$

and a wavelet network approximation $g_N(t)$ is expressed as

$$\begin{cases} g_N(t) = f_N(t), & -l \le t < l \\ g_N(t + 2l) = g_N(t), & \text{otherwise.} \end{cases} \quad (8)$$

In other words, the wavelet network is trained to learn the finite energy function $f(t)$ instead of the original periodic function $g(t)$. In practice, it is not necessary to exactly define the finite energy function $f(t)$. The wavelet network $f_N(t)$ is just trained to approximate some function $f(t)$ that is equal to $g(t)$ in the domain $t \in [-l, l)$ regardless of $t \notin [-l, l)$. In other words, parameters of $f_N(t)$ are updated until $f_N(t)$ approximates $g(t)$ in the domain $t \in [-l, l)$. Hence, the finite energy function $f(t)$ can be any finite energy function that satisfies

$$\begin{cases} f(t) = g(t), & -l \le t < l \\ f(t) = f_N(t), & \text{otherwise.} \end{cases} \quad (9)$$

Besides, the definition of $f(t)$ in the domain $t \notin [-l, l)$ is arbitrary and of no significance during training.

D. Approximation by Periodic Continuous Function

If a periodic function $g(t)$ is continuous, i.e., $g(-l) = g(l)$. As a consequence, its corresponding approximation $f_N(t)$ has to satisfy $f_N(-l) = f_N(l)$. On the other hand, a biased wavelet $h(\tau)$ in (5) decreases quickly and is negligible when $|\tau| > \lambda$, where λ is prescribed as 4 in this paper. The biased wavelets $h(\tau)$ when $|\tau| \le \lambda$ play a major role in approximation. Hence, this paper proposes a wavelet network approximation $f_N(t)$ for periodic continuous functions. The wavelets $h_i((t - b_i)/a_i)$ in $f_N(t)$ have the following characteristics: (i) dilation parameter a_i satisfies $0 < a_i \le l/\lambda$. (ii) translation parameter b_i satisfies $-l \le b_i < l$. (iii) repetitions at translations $b_i - 2l$ and $b_i + 2l$. The wavelets $h_i((t - b_i)/a_i)$ have maximum dilation when the dilation parameter $a_i = l/\lambda$, i.e., $h_i(\lambda(t - b_i)/l)$, and $h_i(t)$ are equal to $h(\lambda)$ at $t = l + b_i$. The wavelet network approximation $f_N(t)$ is defined as

$$f_N(t) = \sum_{i=1}^{N} q_i \left(h_i\left(\frac{t - b_i - 2l}{a_i}\right) + h_i\left(\frac{t - b_i}{a_i}\right) + h_i\left(\frac{t - b_i + 2l}{a_i}\right)\right) + \theta \quad (10)$$

and has $f_N(-l) = f_N(l)$. Parameters in $f_N(t)$ are trained to approximate the finite energy function $f(t)$ defined in (9). The biased wavelet $h(\tau)$ decreases quickly and the value of $h(\tau)$ when $|\tau| > \lambda$ can be treated as zero. Hence, the approximation effect of $h(\tau)$ when $|\tau| > \lambda$ can be negligible and the wavelet sets

$$h_i\left(\frac{t - b_i - 2l}{a_i}\right) + h_i\left(\frac{t - b_i}{a_i}\right) + h_i\left(\frac{t - b_i + 2l}{a_i}\right), -l \le t < l \quad (11)$$

in (10) reduce to $\eta_i(t)$, which is a periodic function defined as shown in (12) at the bottom of the page. The periodic function $\eta_i(t)$ reproduces the major portion of the wavelet $h_i(t)$ with a period $2l$. Truncation of the wavelet $h_i((t - b_i)/a_i)$ leads to $h(\tau)$ with $-l/a \le \tau < l/a$. When the dilation parameter $a_i = l/\lambda$, the major portion of the wavelet $h_i((t - b_i)/a_i)$ is $h(\tau)$ when $-\lambda \le \tau < \lambda$ and equals $h(\tau)$ when a_i tends to become zero. As a result, the wavelet approximation (8) becomes

$$g_N(t) = \sum_{i=1}^{N} q_i \eta_i(t) + \theta \quad (13)$$

where $\eta_i(t)$ are defined in (12).

E. Wavelet Network Controller

According to (13), a WN controller with N nodes in the single hidden layer can be expressed as

$$r_c(t) = \sum_{i=1}^{N} q_i \eta_i(t) + \theta. \quad (14)$$

The WN control signal $r_c(t)$ is a continuous function with a period $2l$ and has an adjustable parameter vector defined as $\boldsymbol{W} = [a_i, b_i, c_i, q_i, \theta]$. The total number of parameters in $\boldsymbol{W}$

$$\begin{cases} \eta_i(t) = h_i\left(\frac{t - b_i}{a_i}\right) = \psi\left(\frac{t - b_i}{a_i}\right) + c_i \cdot \sigma\left(\frac{t - b_i}{a_i}\right), & (-l + b_i) \le t < (b_i + l) \\ \eta_i(t + 2l) = \eta_i(t), & \text{otherwise.} \end{cases} \quad (12)$$

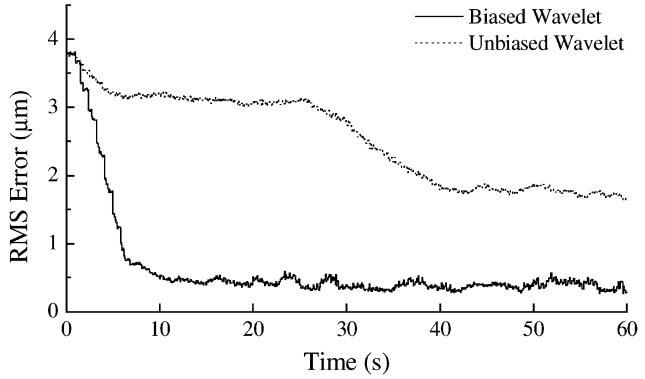

Fig. 4. Comparison of flying height errors during learning using biased and unbiased wavelets.

is $N_W = 4N + 1$. In this paper, a sampling frequency f_s is prescribed as 10 kHz and $\boldsymbol{W}$ can be updated online using a gradient training rule to minimize the error function

$$E = \sum_{k=k_0}^{k_0+4lf_s} e^2(k) \tag{15}$$

where $e(k)$ denotes the system error, k is a sampling step, and k_0 is the initial step in two periods. The error function E is the squared sum of $e(k)$. The parameter w_i is in turn updated to become a new value

$$(w_i)_{j+1} = (w_i)_j - \delta_i \operatorname{sgn}(\Delta E_j) \tag{16}$$

where $(w_i)_{j+1}$ is the updated value of w_i in the jth iteration, ΔE_j is the variation of E and a signum function $\operatorname{sgn}(\cdot)$ determines the training direction of w_i.

In order to examine the stability of the proposed scheme in Fig. 2, a nonnegative function is defined as $V_j = \tilde{\boldsymbol{W}}_{\boldsymbol{j}}^{\boldsymbol{T}} \tilde{\boldsymbol{W}}_{\boldsymbol{j}}$, where $\tilde{\boldsymbol{W}}_{\boldsymbol{j}} = \boldsymbol{W}_{\boldsymbol{j}} - \bar{\boldsymbol{W}}$ denotes in the jth iteration a parameter error vector relative to an optimal parameter vector $\bar{\boldsymbol{W}}$. If the nonrepetitive disturbance $d_{\rm nr}$ is a random distribution during learning and will not affect training direction in (16), V_{j+1} will be limited to the neighborhood of zero; i.e., $\lim_{j\to\infty} V_j \leq \sum_{i=1}^{4N+1} \|\delta_i + \delta_i \alpha_i)\|^2$ where $\alpha_i \geq 0$ is the perturbation of w_i with respect to the nonrepetitive disturbance $d_{\rm nr}$. Hence, parameters are limited to the neighborhood of the optimal parameters and the WN control signal r_c is bounded. For a bounded r_c, the system stability depends on the design of the compensator $C(s)$ in Fig. 2. According to (15) and (16), the gradient training rule will converge slowly if the learning step δ_i is small. However, a large δ_i leads to large oscillation in $\boldsymbol{W}_{\boldsymbol{j}}$. Hence, the learning step δ_i is prescribed as a large constant in the beginning to reduce the system error $e(k)$ quickly. Afterwards, a smaller δ_i is used to improve precision.

F. Simulation Results

Fig. 4 compares learning histories of WN controllers between biased and unbiased wavelets. The latter does without bias parameters, i.e., $c_i = 0$ in (12). The root-mean-square (rms) value of the flying height error is donated as $\operatorname{rms}(e) = \sqrt{E/4lf_s}$.

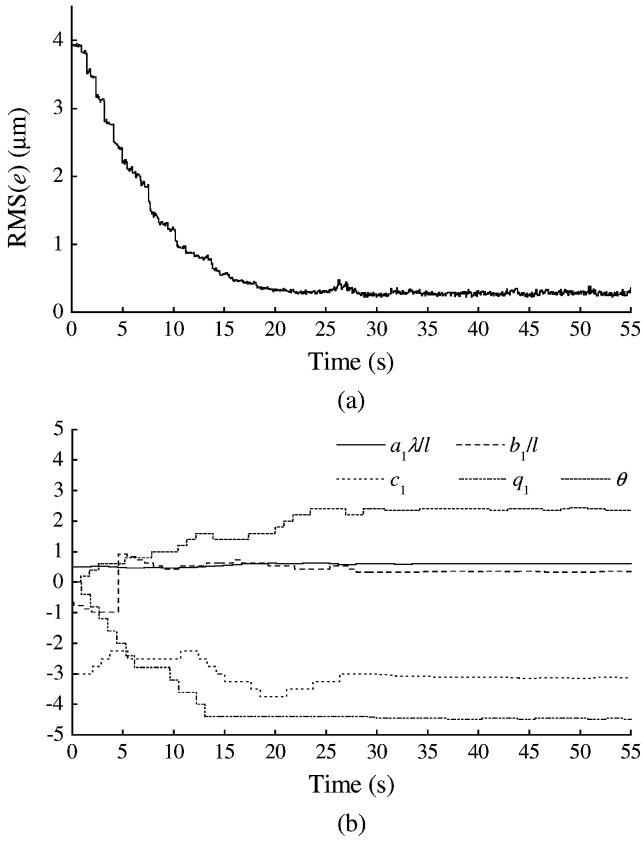

Fig. 5. Learning histories in experiments. (a) $\operatorname{rms}(e)$. (b) a_1, b_1, c_1, q_1, and θ.

Both WN controllers have three neurons in the single hidden layer and have to follow a measured disk surface deformation with peak-to-peak variation of 9 μm at 5400 rpm. Before learning, parameters in the unbiased WN controller are prescribed the same as those in the biased WN controller except c_i. Fig. 4 shows that the biased WN controller not only results in smaller error, but also faster convergence. Hence, the biased wavelet sets are used for WN controllers in experiments.

IV. Experimental Results

In order to demonstrate the effectiveness of the proposed WN controller, experiments are carried out, where a PZT bender is commanded to follow surface deformation of a hard disk rotating at 5400 rpm. A WN is online trained by prescribing a desired flying height $r = r_0$. The WN has three neurons in the single hidden layer. Fig. 5(a) shows that the rms error converges after 20 s. Fig. 5(b) depicts learning histories of the first neuron in the hidden layer, and θ. In the presence of the compensator $C(s)$, the WN controller is not enabled until $t = 5$ s. As shown in Fig. 6, flying height variation rapidly reduces to ± 0.7 μm in 11 ms. Fig. 7 compares power spectrums of the flying height error when the WN controller is disabled and when enabled. As a consequence, the resultant flying height error power reduces 87, 25, and 31 dB at 90, 180, and 270 Hz, respectively, due to the WN controller. Hence, the present WN controller successfully cancels the repetitive disturbance d_r and let the PZT bender follow the disk surface.

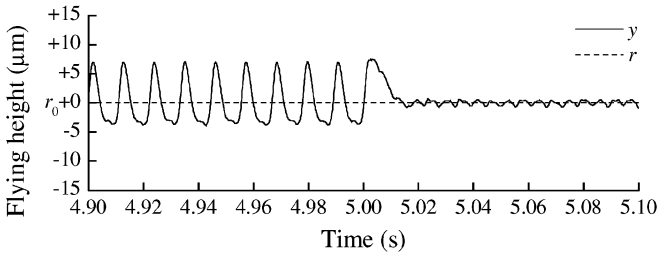

Fig. 6. Measured control results when the PZT bender follows a hard disk with desired flying height r_0.

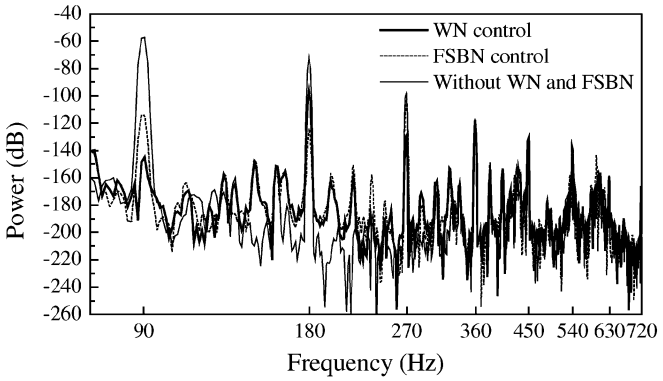

Fig. 7. Comparison of power spectrums for flying height error among WN control, FSBN control, and feedback control without WN and FSBN.

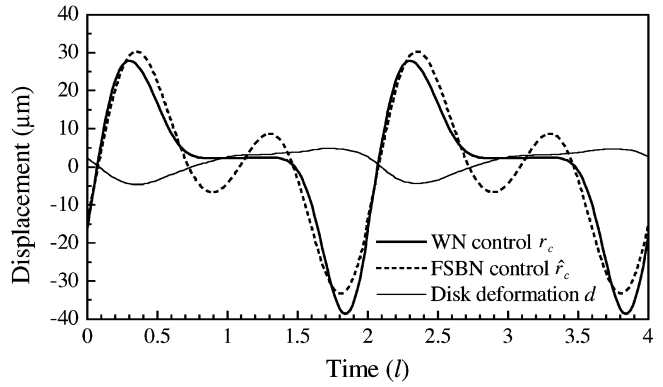

Fig. 8. Comparison of the WN control signal r_c, the FSBN control signal $\hat{r}_c$, and disk deformation d, where l is half period.

In addition to the WN controller, Fig. 7 also compares with a Fourier series-based network (FSBN) controller [9] defined as

$$\hat{r}_c(t) = A_0 + \sum_{n=1}^{M} A_n \cos\left(\frac{n\pi t}{l}\right) + B_n \sin\left(\frac{n\pi t}{l}\right) \quad (17)$$

where $M = 3$ denotes the number of harmonic frequencies; A_0, A_n, and B_n are Fourier coefficients. For comparison, the FSBN controller yields $\hat{r}_c$ that replaces the WN control signal r_c in Fig. 2. The FSBN controller results in a flying height that varies between ± 1 μm in contrast to ± 0.7 μm by using WN. The FSBN controller reduces flying height error power 57, 52, and 5 dB at 90, 180, and 270 Hz, respectively.

The high-frequency repetitive errors at 360 Hz, 450 Hz, etc. have small amplitudes in experimental environment. They are not reduced by WN controllers when more neurons are added in the hidden layer, nor are FSBN controllers with higher order terms $n \geq 4$ in (17).

Fig. 8 compares the WN control signal r_c, the FSBN control signal $\hat{r}_c$, and the measured disk deformation d. The WN control signal r_c leads the disk deformation d by $l/2$, which consists with a 90° phase delay of the open-loop system $KC(s)P(s)$ in the low frequency region as shown in Fig. 3. The FSBN control signal $\hat{r}_c$ behaves similarly to the WN control signal r_c in $t \in [1.5l, 2.7l]$, but oscillates in $t \in [0.7l, 1.5l]$. Therefore, the WN control performs better than FSBN control on the time axis responding to the disk deformation d.

V. Conclusion

Based on a proposed wavelet network, this paper has presented a WN controller to reduce repetitive error in disk drives. The WN controller, which uses the system time in (12) as the only input signal in the input layer, can generate the required control signal that has the same period as the disturbance period. The repetitive error caused by the repetitive disturbance is hence reduced. Experimental results have validated the proposed WN controller, which effectively reduces repetitive flying height error.

References

[1] W. J. Cao and J. X. Xu, "Fourier series-based repetitive learning variable structure control of hard disk drive servos," *IEEE Trans. Magn.*, vol. 36, no. 5, pp. 2251–2254, Sep. 2000.

[2] F. J. Lin and R. J. Wai, "A hybrid computed torque controller using fuzzy neural network for motor-quick-return servo mechanism," *IEEE/ASME Trans. Mechatronics*, vol. 6, no. 1, pp. 75–89, Mar. 2001.

[3] I. Daubechies, "The wavelet transform, time-frequency localization and signal analysis," *IEEE Trans. Inf. Theory*, vol. 36, no. 5, pp. 961–1005, Sep. 1990.

[4] A. Grossmann and J. Morlet, "Decomposition of hardy function into square integrable wavelets of constant shape," *SIAM J. Mathemat. Anal.*, vol. 15, pp. 723–736, 1984.

[5] S. G. Mallat, "A theory for multiresolution signal decomposition: The wavelet representation," *IEEE Trans. Pattern Anal. Mach. Intell.*, vol. 11, no. 7, pp. 674–693, Jul. 1989.

[6] Q. Zhang and A. Benveniste, "Wavelet networks," *IEEE Trans. Neural Netw.*, vol. 3, no. 6, pp. 889–898, Nov. 1992.

[7] B. Delyon, A. Juditsky, and A. Benveniste, "Accuracy analysis for wavelet approximations," *IEEE Trans. Neural Netw.*, vol. 6, no. 2, pp. 332–348, Mar. 1995.

[8] R. K. H. Galvao, T. Yoneyama, and T. N. Rabello, "Signal representation by adaptive biased wavelet expansions," *Digital Signal Process.*, vol. 9, no. 4, pp. 255–240, Oct. 1999.

[9] W. J. Cao and J. X. Xu, "Fourier series-based repetitive learning variable structure control of hard disk drive servos," *IEEE Trans. Magn.*, vol. 36, no. 5, pp. 2251–2254, Sep. 2000.

C. M. Chang received the B.S. degree in mechanical engineering from National Taiwan University of Science and Technology, Taipei, in 1997 and the M.S. and Ph.D. degrees in mechanical engineering from the National Chiao Tung University, Taiwan, in 2000 and 2005, respectively.

Since 2005, he has been with the AU Optronics Corporation (AUO), Taichung, Taiwan. His interests include control, optomechatronics, and display technology.

T. S. Liu received the B.S. degree from National Taiwan University in 1979, the M.S. and Ph.D. degrees from the University of Iowa, Ames, in 1982 and 1986, respectively, all in mechanical engineering.

He has been with Department of Mechanical Engineering, National Chiao Tung University, Taiwan, since 1987. He was a visiting researcher with the Institute of Precision Engineering, Tokyo Institute of Technology, in 1991. He was also a visiting researcher with the Institute of Precision Engineering, Swiss Federal Institute of Technology, Zurich, in 1998. He is currently a Professor with the Department of Mechanical Engineering, National Chiao Tung University. His research interests are in optical disk drives, data storage, and dynamics and control of mechatronic systems.